Volume 11, Issue 7, July – 2026 International Journal of Innovative Science and Research Technology
ISSN No:-2456-2165 https://doi.org/10.38124/ijisrt/26jul1822

Ni(II), Co(III), Cu(II) and Zn(II) Based Complexes with Schiff Base Ligand Synthesis, Characterization and its Antitubercular Activity

Devendra Kumar Singh[1*]; Bipin Bahadur Saxena[2]; Vipin Kumar Singh[3]

[1,2,3]Department of Chemistry, Agra College, Agra, Dr. Bhimrao Ambedkar University Agra, India.

Publication Date: 2026/08/07

Abstract: In the current study, metal ions of Co (III), Zn (II), Cu (II), Ni (II), and Schiff base ligand have been synthesized using a 1:1 molar ratio (3L:M), and (2L:M). To confirm the metal (II) complexes were effectively synthesized, the compound was characterized through UV-Vis, LC-MS, FTIR, elemental analysis, EDX, magnetic susceptibility measurement, and ^{1}HNMR. Its molar conductance confirmed the non-ionic nature of the Co (III), Ni (II), Cu (II), and Zn (II) metal complexes. For these complexes, an octahedral geometry for the Co (III), a square planar geometry for the Cu (II) and Ni(II), and a tetrahedral geometry for the Zn (II) metal complexes have been suggested based on the data displayed. The examined chemicals in vitro biological screening effects were evaluated with respect to the antimicrobial species Klebsiella pneumoniae-7, Klebsiella pneumoniae, Escherichia coli, Proteus mirabilis, Citrobacter amalonaticus, Pseudomonas aeruginosa, Proteus mirabilis-7, Klebsiella pneumoniae, Escherichia coli- 10, and Citrobacter diversus-2, microorganisms species genera, Escherichia Pseudomonas, Citrobacter, Klebsiella and Proteus, and M. tuberculosis species by the agar well diffusion method. A comparison of the inhibitory values of the Schiff base ligands and their metal complexes shows that the complexes have more antituberculous action than the Schiff base ligand. The growth-inhibitor effect has been shown to depend on the metal ions. The initial cell density and the growth medium seemed to have a significant impact on the amount of inhibition.

Keywords: *Schiff Base Ligand, Metal Complexes, FTIR, NMR and Antitubercular Activity".*

How to Cite: Devendra Kumar Singh; Bipin Bahadur Saxena; Vipin Kumar Singh (2026) Ni(II), Co(III), Cu(II) and Zn(II) Based Complexes with Schiff Base Ligand Synthesis, Characterization and its Antitubercular Activity. *International Journal of Innovative Science and Research Technology*, 11(7), 3173-3187. https://doi.org/10.38124/ijisrt/26jul1822

I. INTRODUCTION

In this study, with respect to an extensive number of decades, scientists have been interested in indane-1,3-dione derivatives. Several scientific disciplines have found uses for these compounds, such as non-linear optics (NLO), medicinal chemistry, photo polymerization, organic electronics, and optical sensing. Indanone, one of its closest equivalents, is often associated with the creation of biologically beneficial organic compounds [1-3]. Indandione, based on the altered groups, exhibits several biological characteristics and effortlessly performs several chemical processes that enable the synthesis of novel compounds containing corporate or pharmaceutical qualities [1], and the general structure of indane-1,3-dione.

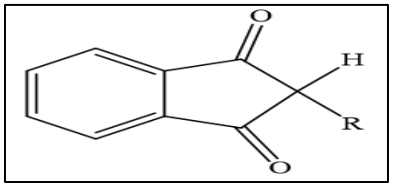

Fig 1 General Structure of Indane-1,3-Dione

Over the last few decades, there has been a greater curiosity towards metallic-based drugs in medicine [1]. The fields of medical chemistry and pharmaceutical research have found enormous use for metals. Metal ions or metals form complexes containing coordination when they bond using ligands [2]. Indeed, upon coordination, they can enhance their biological active profiles with pharmacological ligands, while non-active ligands have the potential to become therapeutic [3-7]. The transition metals, also known as d-block elements, are found in groups III–XII of the periodic table. They exhibit fluctuating oxidation states and partially filled d-orbitals [8]. Furthermore, metal complexes have become significant as inhibitors of proteins because they can either disturb the metals directly or bind firmly to proteins through both ionic and covalent bonds to stop target activities. which can disturb the active site essential for enzymatic action [9-10]. Additionally, one of the most effective methods for creating long-acting or slow-release medications is the use of metal-coordination reservoirs. The metals are important in biological redox processes because of their relative stability in various oxidation states [11]. Metal complexes are widely used as both medicinal and diagnostic agents [8]. Many human diseases like tuberculosis, infection, cancer,

ISSN No:-2456-2165 https://doi.org/10.38124/ijisrt/26jul1822

Alzheimer's disease, and neurological disorders are being treated through metal-ligand complexes [12]. While inorganic Ni(II), Zn(III), Cu(II), and Co(III) salts themselves have shown some activity, the most potent anti-tuberculosis actions are usually reported when Cu(II) Co(III), Ni(II), and Zn(II) are coordinated with specific ligands to form stable complexes [13]. Additionally, several research studies have highlighted the biological characteristics of metal complexes containing oxygen-nitrogen chelating derivatives using multiple carbonyl compounds [14], this compound can potentially bind various organic ligands or mixed ligands to achieve optimal stability and pharmacological performance in vitro, while also exhibiting a broad spectrum of coordination numbers, geometric structures, and specific oxidation states. Several medications function by coordinating with metal ions or inhibiting the synthesis of metalloenzymes [15-16].

The highlighted Publications, inorganic salts of Cu(II), Ni (II), Co(III), and Zn (II) their complexes have significant antimycobacterial and bacteriostatic activity against Mycobacterium tuberculosis [17]. While metal-based treatments (including Ni(II) and other metals) were in widespread use in the pre-penicillin era, recent research has highlighted Cu(II), Ni(II), Co(III), Zn (II) complexes as potential agents to inhibit TB and numerous diseases growth metal complexes, such as Cu(II), Ni(II), Co(III), and Zn(II) 2,6-diacetylpyridine bis(isonicotinoylhydrazonate), [18] showed in vitro anti-tuberculosis activity against M. tuberculosis H37Rv. When Co (III), Cu(II), Ni (II), and Zn(II) are complexed with a ligand such as a Schiff base, the compounds formed often show better anti-TB activity than either ligand alone. [19] Some metal complexes have shown equal or greater activity than standard tuberculosis drugs, such as rifampin or isoniazid, in inhibiting tuberculosis relapses, as observed with certain Cu(II), Zn(II), Co(III), and Ni(II)-hydrazone complexes [20]. Additionally, research suggests that Co(III), Ni(II), Cu(II), and Zn(II) complexation can enhance the activity of well-known anti-tubercular drugs like isoniazid [21], while early anti-tubercular agents contained various metal salts (Cu, Ag, Hg), and Ni(II) complexes remain a hot topic of research today to combat drug-resistant TB and other disease, as demonstrated by their ability to act as multi-target agents [22-23].

Over the past century, the human race has made significant progress in combating viral infections. Fortunately, microorganisms are now able to evade the deadly effects of the majority of these harmful agents; the issue of acquiring tolerance against current antimicrobial agents has become a problem for healthcare professionals [24]. Tuberculosis constitutes one percent the fastest-growing causes of death, affecting people during its most productive years; this contributes to 25% of the total global TB population within India exclusively [25]. The simultaneous development of this illness especially an infection with HIV, together with the recent development of persistently or extremely drug-sensitive tuberculosis (MDRTB and XDRTB) for the initial treatments, creates enormous worldwide problems [26]. The type of bacterial infection known as tuberculosis (TB) is mostly caused by species of Mycobacterium tuberculosis (M. tuberculosis). Lung damage is the main effect of tuberculosis (TB). but it can also damage various parts of the body, which results in symptoms that are not exclusive to the lungs [27–28]. Based on its substantial morbidity and mortality [29], the disease continues to constitute an ongoing worldwide health problem. Outside the lungs, TB occurs in between fifteen and twenty percent of tuberculosis cases, especially in those who are also HIV-positive [30]. Meanwhile, respiratory TB Certain routine investigations have also linked respiratory TB to cancerous lung tumours, and M. TB has been associated with tumour-like forms. It highlights the significance that efficient management has to lowering this risk [31–36]. The risk of contracting the disease significantly increases when medical care for active TB Delaying medical care for active TB significantly increases the risk of contracting the disease. Due to misinterpretation, ambiguous symptoms, and insufficient standardised laboratory capabilities, detecting tuberculosis becomes progressively harder to determine in many cases [38]. Air becomes an important medium for the spread of TB because it carries particles released when an infected person coughs or sneezes [39]. Despite overburdening healthcare systems, disrupting TB treatment, and diverting crucial funds, the COVID-19 pandemic has exacerbated these issues. Clinical outcomes have deteriorated, resulting in increased infections. The overall TB data demonstrates that antimicrobial services have partially recovered, but the long-term consequences of the epidemic continues to hinder progress [40].

Several highlight reports and WHO data show that the number of infections associated with TB reported worldwide throughout the years (2019-2025) has reduced, partially due to restricted access to medical treatment [41]. Global efforts to combat TB have made significant progress. Although there was a partial improvement in 2021, this decrease did not fully account for the missing cases worldwide. However, the COVID-19 pandemic significantly undermined these gains, disrupting TB services around the world [42-45]. The pandemic further exacerbated current inequalities in the availability of medical or therapeutic resources. Low- and middle-income countries, which account for approximately eight percent of TB cases globally, face significant obstacles to establishing World Health Organization (WHO)-approved technologies [46]. There is a nearly 2% decline in the number of people falling ill with TB worldwide, and deaths have decreased by 3% between 2023 and 2024, after increasing for several years (2020–2023) due to the COVID-19 pandemic. Yet in 2024, it remained at a high of 10.7 million [47]. In fact, approximately 10.7 million people worldwide will have tuberculosis (TB) in 2024, and at least 10 million new cases are recorded annually, based on information from the WHO Global Tuberculosis Report 2025, which was published in late 2025 and includes data through 2024 [48]. Most cases are caused by factors such as poor nutrition, HIV and diabetes. Scientists have tried every method to create beneficial compounds that fight disease, while no new chemical entities have become available for treatment in the last forty years [49-50]. But due to problems in treatment and testing, the total number of cases remains high, and TB remains the world's most widespread and deadly disease.

ISSN No:-2456-2165 https://doi.org/10.38124/ijisrt/26jul1822

➢ *Schiff Bases as Ligands, with a Focus on (IBTS):*

The role of Schiff bases as ligands, with a special focus on benzylidine thiosemicarbazide derivatives. Schiff bases (Fig.2) are capable of adaptable compounds composed of υ(C=N), which exhibit physiological activity [51], and the combination of metals in complexes enhances their broadly active, showing anti-inflammatory, antituberculosis, anticancer, antifungal, and antibacterial actions [52-55]. Schiff bases were initially introduced by Hugo Schiff in 1864 [56–60]. In terms of traditional primary amines, most of these compounds are condensation-based derivatives of ketones and aldehydes. They act as flexidentate ligands and coordinate commonly via the N atom of the imine group and O atom of the deprotonated phenolic group [61-62]. Although aliphatic aldehydes are readily polymerized and unstable, aromatic aldehydes possess an excellent conjugated structure and are particularly effective at forming stable Schiff bases [63]. Due to the fact that these compounds containing metal ions are stable, Schiff bases are vital in chemistry [64–65]. Aldehydes are more easily converted to Schiff bases compared to ketones (carbonyl carbon). These ligands have high binding qualities and are simple to synthesise. Given the aforementioned information and the ongoing endeavours to create new compounds to treat tuberculosis [66–68], in the current study, we describe the synthesis and antitubercular activity of α-(1,3-Oxo-Indane-2-yl)-Ethylidine p-bromo aniline and α-(1,3-Oxo-Indane-2-yl)-Benzylidine thiosemicarbazide substituted.

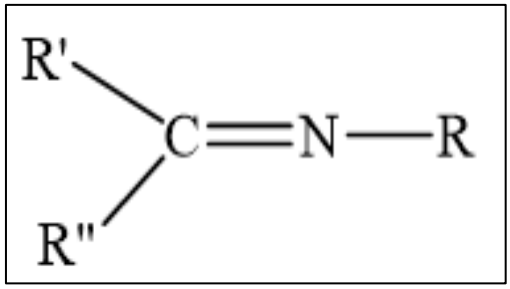

Fig 2 General Structure of Schiff Base

II. EXPERIMENTAL SECTION

➢ *Materials:*

All the compounds specified excellent analysis. 2-Acyl Indane-1,3-dione and p-bromoaniline and 2-Benzoyl Indane-1,3-dione and metal chlorides(MCl_2) were purchased from Sigma-Aldrich Ltd and used without any additional purification. The cup-plate method was used to test the compound's ability to fight tuberculosis at 50, 100, and 200 µg/disc for the biological studies [11]. Sigma Aldrich was the source of the other reagents needed.

➢ *Instrumentations:*

The compound FTIR data were measured using a Perkin Elmer 1600 at Aligarh Muslim University; spectrophotometers with KBr pellets were within the frequency range from 4000 to 400 cm^{-1}. PNMR (400 MHz): the spectrum had been measured on a spectrometer JNM-ECZ400S/L at Aligarh Muslim University; the spectrometer was in d6-DMSO using TMS as an internal reference, and the PNMR spectral data of the Ni(II) complex and its related Schiff base ligand were obtained using the PNMR instrument. The PerkinElmer-Lambda 850 was used to determine the electronic spectral data at Aligarh Muslim University; measurements were made from 200 nm to 800 nm using a spectrophotometer in EtOH solution. Molar conductivity (Λ*m) of a 1 mM EtOH solution was determined using the M K-509 conductivity meter at 25°C, with a complex and ligand. Liquid chromatography mass spectrometer and a solvent (acetonitrile), Aligarh Muslim University; spectrometer on a Triple TOF 5600+, make-Sciex. Kofler apparatus (Nageman, Germany) were uncorrected and utilized to calculate melting points. The compounds were examined for symptoms associated with biological activity. The JNU medical college conducted the assay at AMU, Aligarh. Element analysis for C, N, and H was carried out and calculated on the (SEM) Model No. JSM 6510 LV. The metal complexes' magnetic susceptibility was determined by Gouy's method, Model No. 7641C, with $[HgCo(SCN)_4]$ as the standard; Physics Department, Aligarh Muslim University. XRD data were calculated using a Perkin Elmer 1600 at the Department of Chemistry, AMU, Aligarh.

➢ *Preparation and Characterization of Ligand(L_1 & L_2):*

The Schiff base ligand was synthesised through refluxing an equivalent amount of 2-acyl indane-1,3-dione and p-bromoaniline, 2-Benzoyl Indane-1,3-dione and thiosemicarbazide in a 50 ml ethanol solution for three hours in a round-bottom flask at the 20.50°C temperature. The round-bottom flask then separated and settled, and when it cooled to room temperature, the whitish-coloured precipitate formed and the ethanol evaporated. The purified precipitate was checked by TLC. yield 81.56%; m. p.: 20.50°C. Anal. Calc. for $C_{17}H_{12}O_2NBr$ (m. wt. = 341.904): C = 59.66(60.21), H = 3.50(3.01), O = 9.35(8.89), N = 4.09(3.97), Br = 23.37(22.23); FTIR (KBr, cm^{-1}): 1760 υ(C = O), 1654 υ(C = N), 1486 υ(C = C), and 673 – 584 υ(C – Br) [69-70,]; λmax = 320 nm and λmax = 475 nm [71]; 1H-NMR (DMSO-d6): 1.3 (s, 3H, CH_3), 3.9 (s, 1H, C_2-H), 8.0 (d, 2H, C_4-H & C_7-H), 8.3 (m, 2H, C_5-H & C_6-H), 7.5 (d, 2H, C_2-H & C_6-H), and 7.8 (d, 2H, C_3-H & C_5-H); LC-MS: m/z [M] = 341.904 and m/z $[M_1^+]$ = 342.000 [69], and yield 80.40%; 22.50 ^{0}C. Anal. Calc for $C_{17}H_{13}O_2N_3S$ (m. wt = 323.000): C = 62.80(63.41), H = 3.88 (4.05), O = 8.63(9.50), N = 12.55(12.99), S = 3.75(2.44)%; FTIR(KBr, cm^{-1}): 1771 υ(C = O), 1624 υ(C =N), 3144 υ(N-H), 1482 υ(C =C), and 1226 – 1425 υ(C =S) [69-71]; λmax = 275 nm and λmax = 295 nm [72]; ^{1}H-NMR(DMSO-d_6): 10.5(s, 1H, NH), 2.8(s, 2H, NH_2), 7.9(d, 2H,C'$_2$-H & C'$_6$-H), 7.5(m, 2H, C'$_3$-H & C'$_5$-H), 7.7 (m, 1H, C'$_4$-H), 8.0 (d, 2H, C_4-H &C_7-H), 8.3 (m, 2H, C_5-H & C_6-H); LC-MS: m/z $[M_1^+]$ = 324.3145 and m/z $[M_2^+]$ = 325.3148 [69,73].

ISSN No:-2456-2165 https://doi.org/10.38124/ijisrt/26jul1822

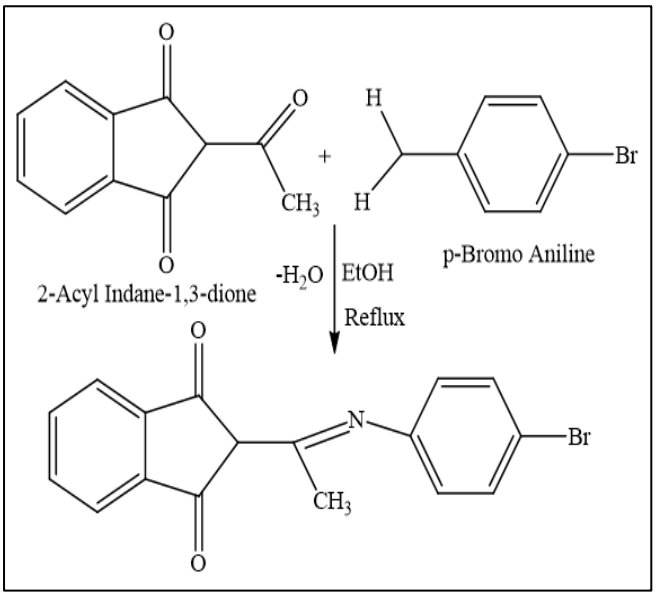

Fig 3 Structure of Schiff Base Ligand (IEPBA)

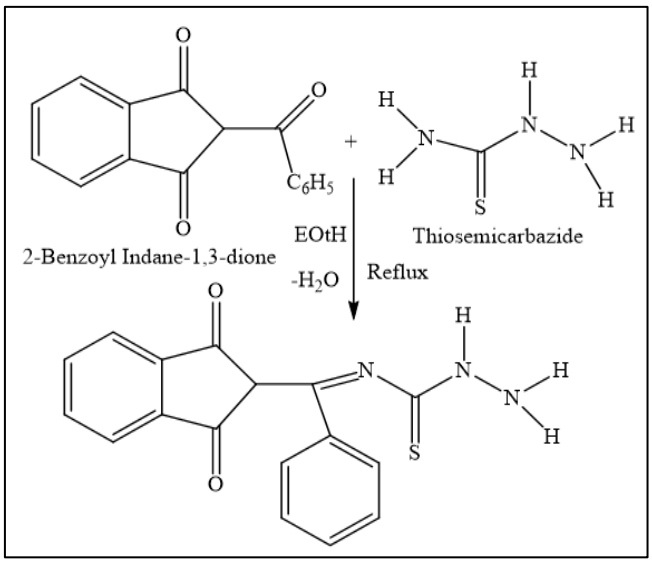

Fig 4 Structure of Schiff Base Ligand (IBTS)

➢ *Preparation of Metal Complexes:*

In 50 ml of ethanol, Co(III) chloride, Cu(II) chloride, Ni(II) chloride, Zn(II) chloride, and Schiff base ligand (1M:3L mmol) and (1M:2L mmol) were dissolved and rapidly shaken. With continuous constant stirring, the Schiff base ligand and metal complex solution gradually developed without any temperature adjustments. The Co(III) metal complex produced a dusty pink precipitate, which was stored in a quiet place for 15 to 16 hours. The chinese rose-colored precipitate was produced after 16 hours, replacing the dusty pink color. After that, the same processing on the Cu (II), Ni (II), and Zn (II) metal complexes for 15, 17, and 14 hrs., respectively, precipitates with reddish-brown, yellow-green, and white colors were produced. These precipitates were then dried at room temperature; the solid was soluble in ethanol, methanol, and acetone but insoluble in benzene and chloroform. The TLC method; the purity is checked.

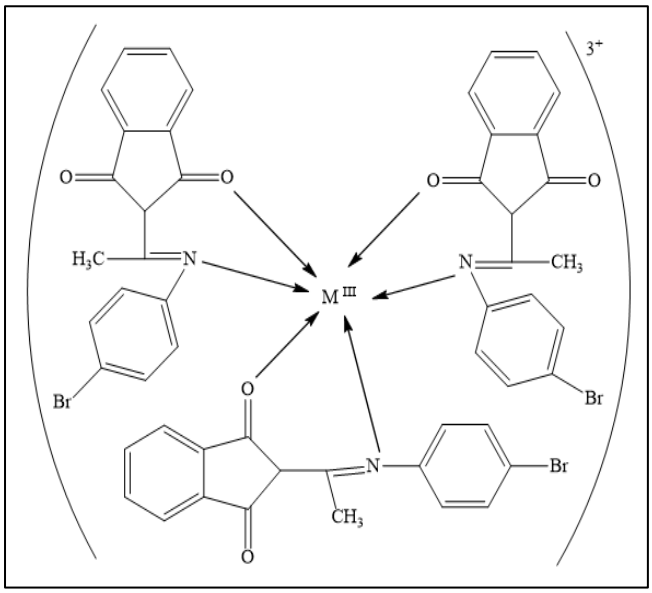
Fig 5 Structure of Metal Complex [M ^{III} = Co (III)]

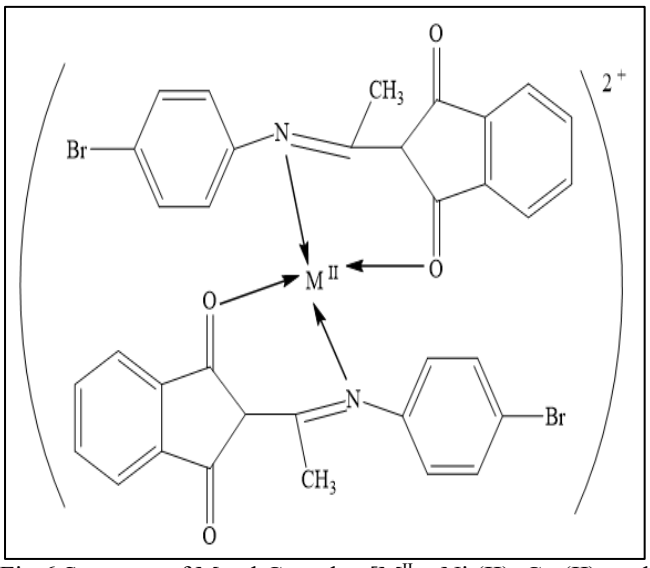
Fig 6 Structure of Metal Complex [M^{II} = Ni (II), Cu (II), and Zn (II)]

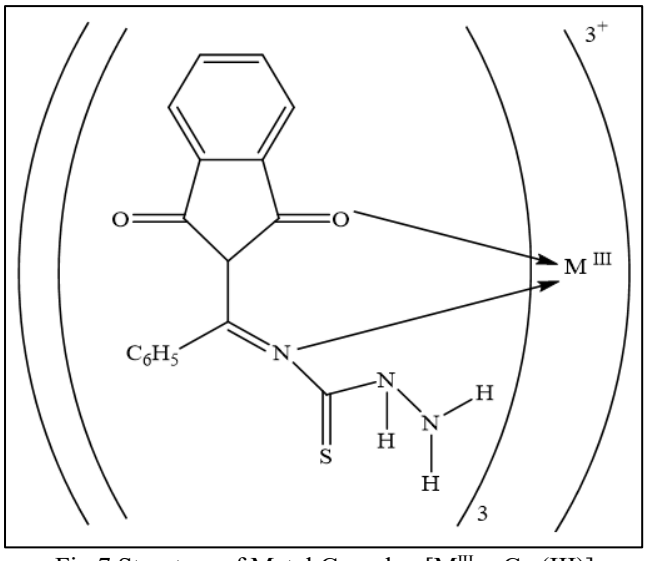
Fig 7 Structure of Metal Complex [M^{III} = Co (III)]

ISSN No:-2456-2165 https://doi.org/10.38124/ijisrt/26jul1822

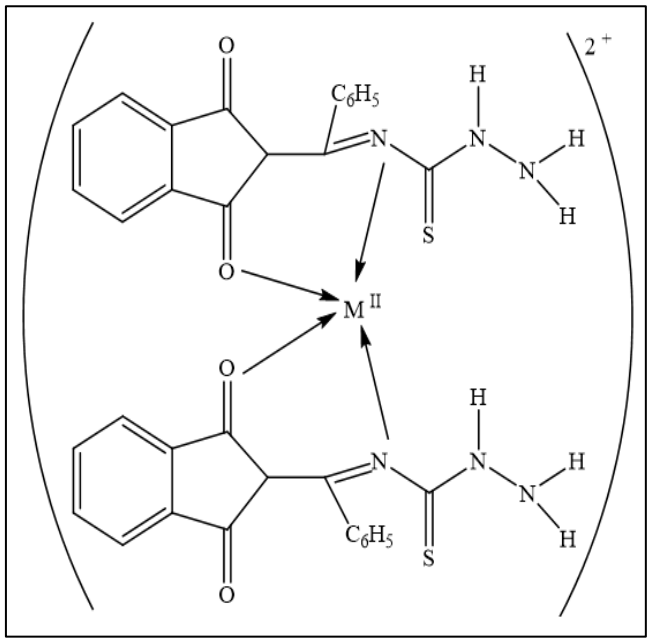

Fig 8 Structure of Metal Complex [M^{II} = Ni (II), Cu (II), and Zn (II)]

➢ *Synthesis of Metal Complex:*

- *[Co(III)L_1]*

m.p.: 20 ^{0}C; Anal. Calc. for $(C_{17}H_{12}O_2NBr)_3Co$ (m. wt. = 1084.402): Yield: 77%, FTIR (KBr, cm^{-1}): 1770 υ(C=O), 1616 υ(C=N), 1497 υ(C=C), 632-551 υ(C-Br), 1324-1435 υ(C-CH3); υCo←O 530, υCo←N 422 [69,73]; Metal content (%) Observed: Co = 5.09(5.43), O = 8.34(8.84), N = 3.29(3.87), H = 3.00(3.35), C = 55.83(56.43); Molar conductivity(m): 16.55 (cm^2/Ω^1 mol^1, alcohol) at 25 ^{0}C; λmax = 298 nm and λmax = 455 nm [73]; magnetic susceptibility value(μeff/μB) = 0 [74].

- *[Ni(II)L_1]*

m.p: 25^{0}C; Anal. Calc. for $(C_{17}H_{12}O_2NBr)_2Ni$ (m. wt. = 742.498): Yield: 79%, FTIR (KBr, cm^{-1}): 1771 υ(C=O), 1634 υ(C=N), 1486 υ(C=C), 642-520 υ(C-Br), 1390-1425 υ(C-CH_3); υNi←O 519, υNi←N 418 **[** 69,73**];** Metal content (%) Observed: Ni = 6.86(7.90), N = 3.49(3.77), O = 7.76(8.61), H = 3.10(3.26), C = 55.84(54.96), Br = 20.54(21.51); Molar conductivity(m): 14.50 (cm^2/Ω^1 mol^1, alcohol) at 25^{0}C; magnetic susceptibility value(μeff/μB) = 0 [74]; λmax = 295 nm and λmax = 450 nm [73].

- *[Cu(II)L_1]*

m.p.: 24 ^{0}C; Anal. Calc. for $(C_{17}H_{12}O_2NBr)_2Cu$ (m. wt. = 747.354): Yield: 77%, FTIR (KBr, cm^{-1}): 1709 υ(C=O), 1614 υ(C=N), 1488-1445 υ(C=C), 648-510 υ(C-Br); υCu←O 515, υCu←N 414 [69,73,75]; Metal content (%) Observed: Cu = 7.01(8.50), H = 3.01(3.23), N = 3.15(3.75), O = 7.91(8.56), Br = 20.88(21.37); Molar conductivity(m): 15.65 (cm^2/Ω^1 mol^1, alcohol) at 25 ^{0}C; λmax = 340 nm and λmax = 444 nm [73]; magnetic susceptibility value(μeff/μB) = 1.79-1.84 [73];

- *[Zn(II)L_1]*

m.p.: 25 ^{0}C; Anal. Calc. for $(C_{17}H_{12}O_2NBr)_2Zn$ (m. wt = 820.294): Yield: 80%, FTIR (KBr, cm^{-1}): 1764 υ(C=O), 1679-1564 υ(C=N), 1486 υ(C=C), 1334-1456 υ(C-CH3); 663-530 υ(C-Br); υZn←O 514, υNi←N 423 [69.76]; Metal content (%) Observed: Zn = 7.07(7.97), O = 8.04(7.80), N = 3.01(3.14), C = 50.64(49.73), H = 2.44(2.92), Br = 20.90(19.48); Molar conductivity(m): 17.60 (cm^2/Ω^1 mol^1 alcohol) at 25 ^{0}C; magnetic susceptibility value(μeff/μB) = 0 [75]; λmax = 342 nm and λmax = 441 nm [73].

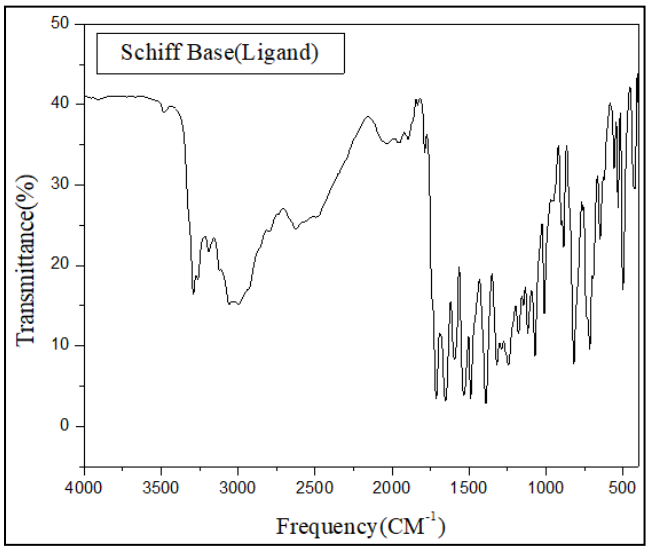

Fig 9 FTIR Structure of Ligand-1

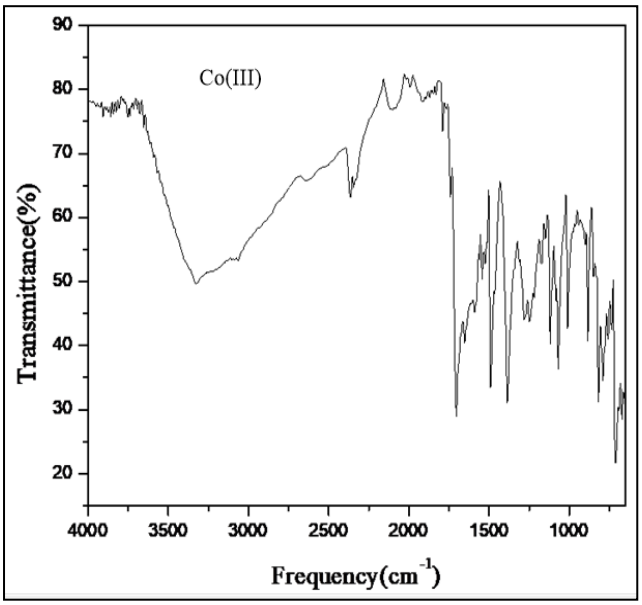

Fig 10 FTIR Structure of Co (III) Metal

ISSN No:-2456-2165 https://doi.org/10.38124/ijisrt/26jul1822

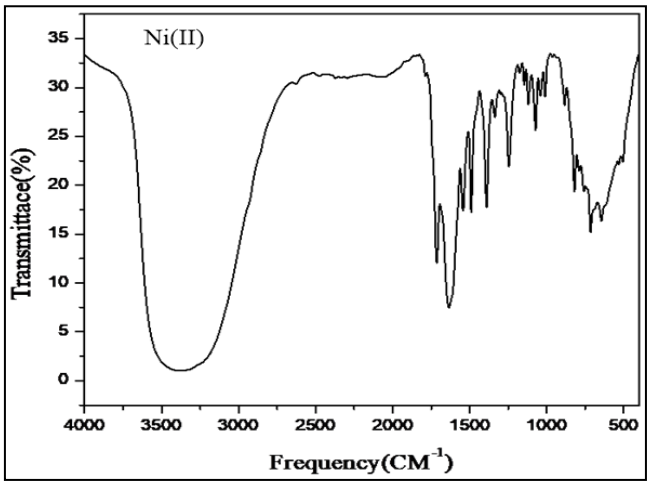

Fig 11 FTIR Structure of Ni(II) Metal

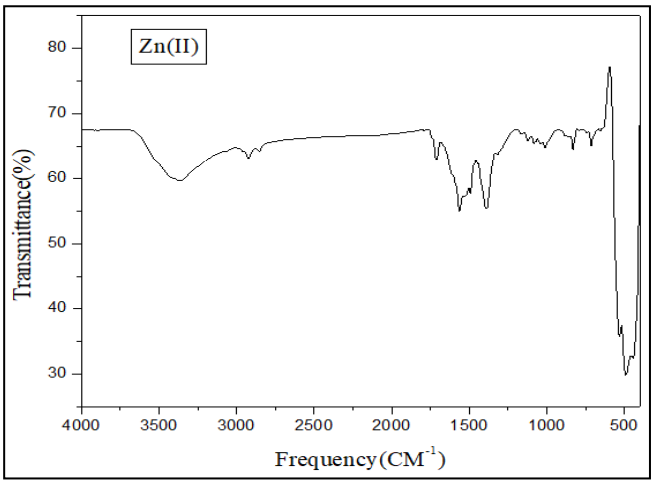

Fig 13 FTIR Structure of Zn(II) Metal

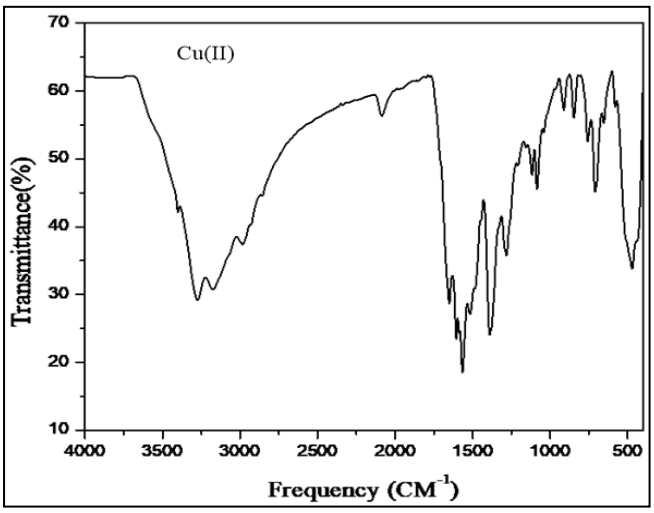

Fig 12 FTIR Structure of Cu(II) Metal

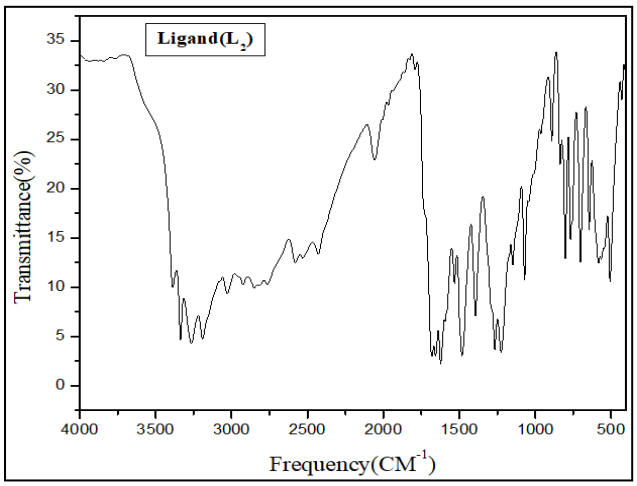

Fig 14 FTIR Structure of Ligand-2

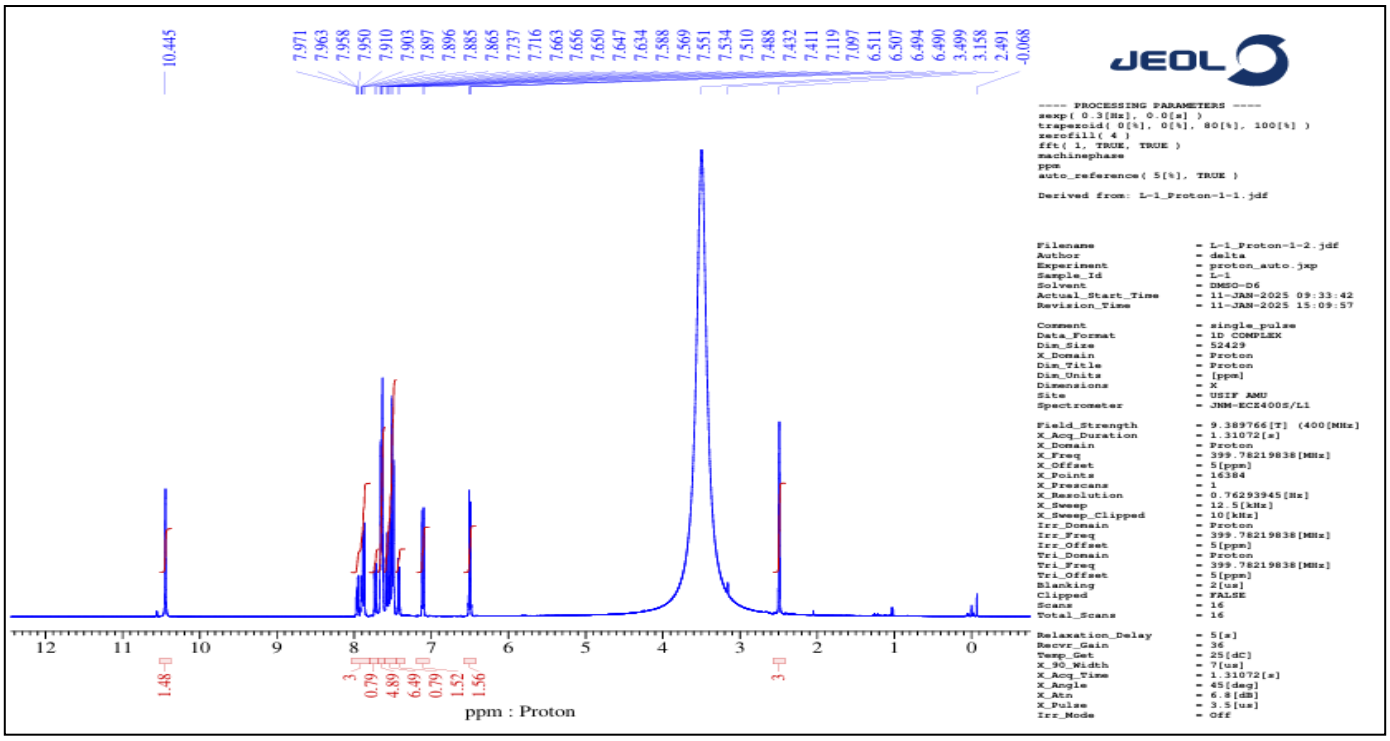

Fig 15 Structure of NMR Ligand- 1

ISSN No:-2456-2165 https://doi.org/10.38124/ijisrt/26jul1822

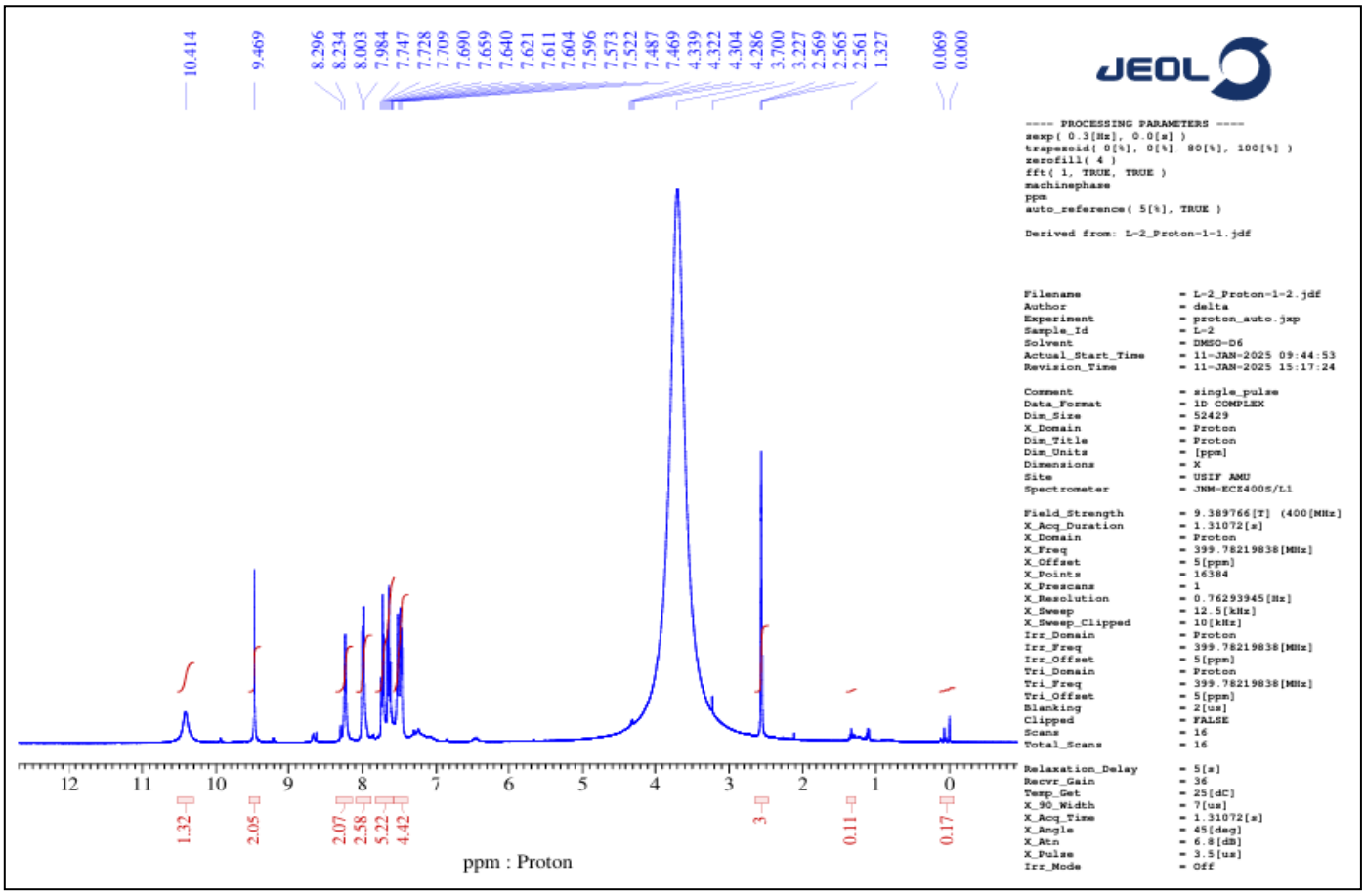

Fig 16 Structure of NMR Ligand-2

III. BIOLOGICAL ACTIVITY ASSESSMENT

➢ *Microorganisms:*

Microorganisms from the genera Escherichia pseudomonas, Klebsiella, Citrobacter, and Proteus which create ESBL and MBL were used to assess antimicrobial activity (Table 3). According to previous studies, these types of isolates were gathered from pathological labs and community-based hospitals, and their MBL/ESBL features were assessed [76, 23]. Meanwhile, the H37Rv strain of M. tuberculosis (ATCC No. 27294) was selected for the assessment of its antitubercular activity in vitro.

The MBL and ESBL-producing bacteria from the Citrobacter, Klebsiella, Proteus, and genera Escherichia pseudomonas, were used to assess antimicrobial activitives (Table 3). These isolated samples were gathered from community-based medical institutions and pathological labs, and their MBL/ESBL characteristics were evaluated [76, 23]. Meanwhile, the H37Rv strain of M. tuberculosis (ATCC No. 27294) was selected to determine its antitubercular activities in vitro.

➢ *Antimicrobial Assessment:*

The DMSO solution was used as a solvent in the agar well-diffusion method [77, 24] to measure the antibacterial activity. Assuming an ultimate concentration of 25 µg/µl, the compounds were evaluated. Test isolates were inoculated in 10 millilitres of BHI (Brain Heart Infusion) broth and incubated at 37°C for a day to produce actively developing log-phase cultures. A 0.4 ml test culture was used to seed Muller-Hinton agar media (20 ml), which were then added to each 9 cm-diameter Petri plate. After allowing the medium to set, every plate had wells drilled using a sterile cork borer. After adding 50 µl of test compounds to each well, the plates were sealed. These plates were incubated at 37°C for 24 hours. 50 µl of DMSO solution was used to create control wells. In order to report zones of inhibition [78, 25], all observations were taken in three sets.

➢ *Antitubercular Assessment:*

The highlighted every phase, and synthesised compounds were evaluated by antitubercular screening performed using the Microplate Alamar Blue the assay being performed. A conventional remedy containing 1000 parts per million of each individual constituent was created. The usual solution was used to create the corresponding standard reagent solutions at concentrations ranging from 0.8 µg/ml to 100 µg/ml. A clean, sterilised 96-well plate was filled with the test solution, 200 µl of pure deionised water, and 100 µl of Middlebrook 7H9 broth. The resulting plate was sealed and allowed hatching to take place at 37ºC over five days. Furthermore, 25 µl of Tween (10 & 80 percent) and Almar Blue (1:1 ratio) were added to each well, and the mixture was incubated for a day. The Minimum Inhibitory Concentration (MIC) for Mycobacterium growth was found to be pink, while no bacterium growth within the well was indicated due to blue colouration [79, 26].

ISSN No:-2456-2165 https://doi.org/10.38124/ijisrt/26jul1822

IV. RESULTS AND DISCUSSION

➢ *Characterization of Ligands (L_1 &L_2):*

The (IEPBA & IBTS) and 2-Acyl-Indane-1,3-dione, and 2-Benzyl-Indane-1,3-dione derivatives condensed in a 1:1 molar ratio to create Schiff bases. The ^{1}HNMR spectra obtained in a DMSO-d_6 solvent provide evidence for this. Two peaks in the ligand's(IEPBA) NMR spectra were identified as belonging to the imine proton in the region of δ 7.50.00-7.80 ppm and the hydroxyl proton in the range of δ 8.00-8.30 ppm. The primary imine proton of IEPBA is responsible for the singlet between 1.30 and 3.90 ppm, and another ligand(IBTS) which identified as belong to the imine proton in the region of δ 7.5 – 7.9 ppm, and carbonyl proton in the range of δ 8.0 – 8.3 ppm, and the amine proton of IBTS is responsible for the singlet between 2.8 ppm & 10.0 ppm, which vanished, indicating the creation of Schiff base. The ligands' FTIR (IEPBA) spectra showed distinctive absorption bands for the carbonyl and imine groups at 1760, 1654 cm^{-1}, and 1486 cm^{-1}, and (IBTS) spectra 1771 cm^{-1}, 1624 cm^{-1}, 3144 cm^{-1}, 1482 cm^{-1}, and 1226-1425 cm^{-1} respectively. The phenolic group caused a wide band to appear in the 3208–3006 cm^{-1}, and 3264 – 3057cm^{-1} range. The anticipated free -OH stretching frequency of 3622–3521 cm^{-1}, and 3706 – 3390 cm^{-1}, and is higher than this figure. This is because phenolic -OH, imine nitrogen, and carbonyl generate strong O-H-N-type hydrogen bonds. The two corresponding tautomeric compound forms, quinoneamine and phenolimine, have been generated as a result of this particular sort of functional hydrogen bonding. However, the carbonyl can only draw a little amount of phenolic -OH in comparison to imine nitrogen. As a result, the carbonyl frequency in the ligand(IEPBA) spectra is found to be comparatively higher (1760 cm^{-1}) than in the free imine (1654 cm^{-1}), and ligand(IBTS) spectra 1771 cm^{-1} υ(C = O) and 1624 cm^{-1} υ(C = N) [69-70, 71]. Additionally, the mass spectrum showed predicted molecular ion peaks for Schiff base ligands HL_1 and HL_2, corresponding to [M^{+}_1] at m/z = 342.000 and [M^{+1}] at m/z = 324.3145, respectively. The phenol mine form of the ligand was shown by the UV-visible spectrum of HL_1 and HL_2 in alcohol, which showed prominent bands caused by n→π* and π→π* transitions in the region of 320 nm and 475 nm, 275 nm, and 295 nm [77].

➢ *Ftir Spectral Studies:*

The infrared spectra of Schiff's base ligand and complexes revealed several vibrational modes of varying intensities in the 4000–400 cm−1 range. Table 1 shows the primary stretching frequencies of the ligand and their complexes.

The metal-ligand bonding is indicated from multiple groups found in the FTIR spectra of the metal Co (III) complexes. Stretching vibrations of the υ(C–H) (aryl group) may be responsible for the FTIR band at 3093 cm^{-1}. For this –CH_3 groups υ(C–H) frequency, the strong and clear FTIR band at 1324–1435 cm^{-1} can be used as a reference [78]. The strong bands at 1770 cm^{-1} may be caused by its υ(C=O) (carbonyl) frequency [69, 72]. A complex coordination between the carbonyl group υ(C=O) and a metal ion is indicated when the carbonyl group is absorbed at a frequency lower than the free υ(C=O) frequency. Further analyzed are the FTIR absorption bands for the υ(C=C) (benzene ring) band at 1497 cm^{-1} [80], the υ(C=N) imine group frequency at 1616–1435 cm^{-1} [72, 73], and the υ(C –Br) frequency at 632–551 cm^{-1} [79]. Both nitrogen and oxygen atoms were found to be involved in the formation of a coordination bond between the Co(III) ion and carbonyl and imine groups. On the other hand, Ni (II) metal ions, the strong bands at 1771 cm^{-1} can be attributed to the υ(C=O) (carbonyl group) frequency and the bands at 1634 cm^{-1} to the υ(C=N) (imine group) frequency. The metal Cu(II) 1709 υ(C=O), 1614 υ(C=O), and Zn(II) 1679-1564 cm-1 can be used as references for this frequency [69, 80-81].

Table 1 Characteristic FTIR Peaks:

Tentative Assisgnments	Compounds(CM^{-1})					
	HL_1	HL_2	[$Co(L_1)Cl$]	[$Ni(L_1)Cl$]	[$Cu(L_1)Cl$]	[$Zn(L_1)Cl$]
υ(OH)	3208-3006	3264-3067				
υ(C=O)	1760	1771	1770	1771	1709	1764
υ(C=N)	1654	1624	1616	1634	1614	1679-1564
υ(C=C)	1486	1482	1497	1486	1488-1445	1486
υ(C - Br)	673-584	-	632-551	642-520	648-510	663-530
υ(C= S)	-	1425	-	-	-	-
υ(N - H)	-	3144	-	-	-	-
υ(M←O)	-	-	530	519	515	514
υ(M←N)	-	-	422	418	414	423

➢ *Electronic Spectral Studies:*

At room temperature, the UV-Vis spectrum that the ligand and it's metal complex in EtOH and range 250-600 nm. Two absorption bands were observed in the ligand electronic spectra at wavelengths of 320, and 475 nm [69,73].

In addition, the electromagnetic spectrum characterisation of the China-rose Co(III) colour complex has demonstrated that $(C_{17}H_{12}O_2NBr)_3Co$ is a six-coordinated Co(III) complex. The electronic spectra showed two absorption bands moved toward lower (298 nm) and higher (455 nm) frequencies; the complex's decreased symmetry from normal, typical octahedral geometry might be the reason for this split [72]. While observing the electronic spectra of the soft yellow-green Ni(II) colour complex revealed two transition bands at 295 nm and 450 nm frequencies. The complex symmetry dropping from square planar geometry [72] and the dark brown Cu(II) colour complex presumably

ISSN No:-2456-2165 https://doi.org/10.38124/ijisrt/26jul1822

contributed to causing these bands to move towards lower and higher frequencies. In the electronic spectra, two transition bands were found at 340 nm and 444 nm [72]. These bands moved to lower and higher frequencies. One possible explanation for this split is that the complex symmetry decreased from square-planar geometry, and the Zn(II) complex has a white-coloured electronic spectrum. As the electronic spectra demonstrated, two transition bands have been observed: 342 nm and 441 nm [72]. Then these bands shifted towards lower (342 nm) and higher (441 nm) frequencies. This breach may be caused by the complex's symmetry diminishing from tetrahedral geometry, which is common for different coordination groups [72,82,83], while d⟶d transitions were identified as the cause of the third band. This separation could be attributed to the n–π* and π⟶π* transitions of the carbonyl (C=O) and imine (C=N) groups, or aromatic rings, which are intra-ligand charge transfer (ILCT) transitions. It may also be caused by a decrease in the complex's symmetry from square-planar/tetrahedral geometry, which is anticipated in various coordination groups, thereby. The charge transfer (CT) transitions are then likely a combination of metal-to-ligand (ML) and ligand-to-metal (LM) transitions.

➢ *Antimicrobial Activity:*

A comparison of the antibacterial activity of gram-negative uropathogens with zones of 14-21 mm against all synthesised compounds using the agar well-diffusion method was conducted using a combination of multidrug-treated and isolated species that are sensitive towards antibiotics (Table 3), particularly immunity to these medications of 3rd generations (Table 4) illustrates the antibacterial activity of all medicines and DMSO (solvent) as a zone of inhibition (mm). With the exception of pneumoniae-7, K. uropathogens, and P. aeruginosa which showed identical spots where the ligand and their metallic complexes are inhibited, metal complexes demonstrated significantly larger zones of inhibition compared to the free ligand, with zones of 14–21 mm. In comparison to Ligand HL_1 and its transition metal complexes, Ligand HL_2 and its resulting complexes exhibited greater antibacterial activity. Considering a location of anxiety ranging from 11 to 21 mm, Cu(II) and Zn(II) complexes demonstrated outstanding antibacterial effectiveness towards every test isolated specimens. as and were established comparatively much more accurate than Ni(II) and Co(III) complexes. With the exception of P. mirabilis, K. pneumoniae, and, E. coli-10 which showed no zone of inhibition, cobalt complex $[Co(L_1)Cl]$ showed zones of inhibition of 11–14 mm. Despite significant zones of inhibition (11–21 mm) against a large proportion of microorganisms, cobalt complex $[Co(L_2)Cl]$ was determined to be the most active chemical. With the exception of P. mirabilis-7, C. diversus-2, K. pneumoniae, and nickel complex $[Ni(L_1)Cl]$ showed significant zones of inhibition of 10–13.5 mm, whereas $[Ni(L_2)Cl]$ showed zones of inhibition of 11–12.5 mm with the exception of K. pneumoniae, P. mirabilis-7, E. coli, and P. mirabilis. Together with zones of 14–21 mm in size, all of the drugs showed the highest inhibitory action against C. amalonaticus MBL uropathogens, while K. pneumoniae ESBL uropathogens showed the lowest antimicrobial activity. Significant antibacterial action was demonstrated by the compounds $[Cu(L_2)Cl]$, $[Co(L_2)Cl]$, $[Cu(L_1)Cl]$, and [Ni $(L_2)Cl$]. These compounds can be utilised to both increase and successfully overcome resistance to drugs.

The strengthened antimicrobial impact of metal-coordinating spots on microorganism enzymes, which reduces the growth of these microorganisms compared to the ligands, can be attributed to the concepts of Cell permeation, and theory of chelation. The antibacterial action of the metal-coordinating sites on microorganism enzymes is heightened by the detection of the electron-removing group within the aromatic ring. Consequently, the microscopic organism complex's development was lower than that of the complex without any replacement [84]. The path of the lipid-soluble chemical is regulated by the lipid permeability for the membrane surrounding the micro-organism cell. Together with the donating group, the metallic ions demonstrates a charge that is positive as a result of ion exchange. As a result, the orientation of the metallic ion is reduced, and there is a higher probability that π-electrons will delocalize throughout the entirety of a metal complex ring. This process makes the metal complex more lipophilic, which enables the metal compound to effectively penetrate the lipid barrier and conceal the metallic-coordinating spots on microorganism enzymes. thereby reducing their growth. Additionally, it has been discovered that metal-based compounds affect microorganisms' respiratory cycle rate primarily preventing the synthesis of proteins. which leads to cell death and growth restriction [85].

Table 2 Multidrug-Resistant Microbial Cultures:

Type of culture	Codename	Complete name
MBL	618	Klebsiella pneumonia
	607	Proteus mirabilis
	220	Escherichia coli
	135	Citrobacter amalonaticus
	85	Pseudomonas aeruginosa
ESBL	Pro-7	Proteus mirabilis-7
	Kp-7	Klebsiella pneumoniae-7
	Kp	Klebsiella pneumonia
	Ec-10	Escherichia coli- 10
	Citro-2	Citrobacter diversus-2

ISSN No:-2456-2165 https://doi.org/10.38124/ijisrt/26jul1822

Table 3 Antimicrobial Activity:

Sr. No.	Compounds	Zone of Inhibition (mm)									
		ESBL					MBL				
		Citro-2	Ec-10	Kp	Kp-7	Pro- 7	85	135	220	607	618
1	DMSO (Solvent)	0	0	0	0	0	0	0	0	0	0
2	HL_1	0	0	0	11.5	0	11	14.5	0	0	0
3	$[Co(L_1)Cl]$	11	0	0	11.6	13	11	14.5	0	0	12
4	$[Ni(L_1)Cl]$	0	10	0	12	0	13.5	13.6	10.5	11.5	11.5
5	$[Cu(L_1)Cl]$	15	11	11.5	11	12	12.5	15	15.5	12.5	11
6	$[Zn(L_1)Cl]$	14	11	11.6	11.5	12	10.5	15	11.4	11.5	10.5
7	HL_2	0	12	0	11.5	0	12	13.5	0	0	11.5
8	$[Co(L_2)Cl]$	21	11	0	13	14	14.5	22	13	14	17.5
9	$[Ni(L_2)Cl]$	11	12	0	11	0	12.5	12.5	0	0	11.5
10	$[Cu(L_2)Cl]$	16	14	12	12	14.5	13	19.5	16	15	11
11	$[Zn(L_2)Cl]$	10.5	14	12	10.5	11.6	15	17.6	11	11.5	12

➢ *Antitubercular Activity:*

The standard pharmaceutical drugs like Streptomycin, Ciprofloxacin, and Pyrazinamide were used to determine the antitubercular performance associated with all produced compounds against M. tuberculosis. Every compound was shown to be effective against M. tuberculosis, as illustrated in table 4 and Fig.17**.** To effectively break through the extremely thick, wax cell wall of M. tuberculosis, an antitubercular medication needs to be sufficiently lipophilic [86]. Schiff base ligands HL_1 and HL_2 showed lower activity (MIC=50.0 µg/ml) when corresponding to the respective metallic compounds. This type of activity could be explained through the formation of metallic chelate structures, which have better lipophilic qualities than Schiff base ligands and allow the metal complex to pass through the dense microbe-based cell membrane with greater effectiveness, resulting in bettered antitubercular action [87-91]. In comparison with Co(III), Zn(II), and Ni(II) compounds, Cu(II) and Ni(II) compounds demonstrated greater activity against M. tuberculosis. Copper complexes $[Cu(L_2)Cl]$ and $[Cu(L_1)Cl]$ and zinc complexes $[Zn(L_1)Cl]$ displayed high antitubercular activity, while Co(III) and Ni(II) complexes demonstrated justifiable antitubercular activity [92-93].

Table 4 Antitubercular Activity:

Test compound	MIC (µg/ml)
*Pyrazinamide**	3.11
*Ciprofloxacin**	3.11
*Streptomycin**	6.26
HL_1	50.0
HL2	50.0
$[Co(L_1)Cl]$	50.0
[Ni(L1)Cl]	25.1
[Co(L2)Cl]	25.1
[Ni(L2)Cl]	25.1
[Zn(L2)Cl]	25.1
$[Cu(L_1)Cl]$	12.4
$[Zn(L_1)Cl]$	12.4
[Cu(L2)Cl]	12.4

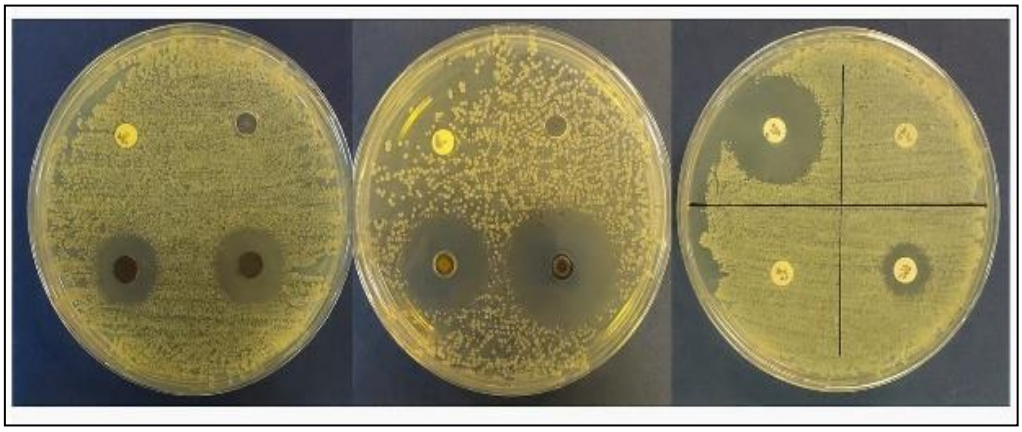

Fig 17 Test Compounds Plate Photo

ISSN No:-2456-2165 https://doi.org/10.38124/ijisrt/26jul1822

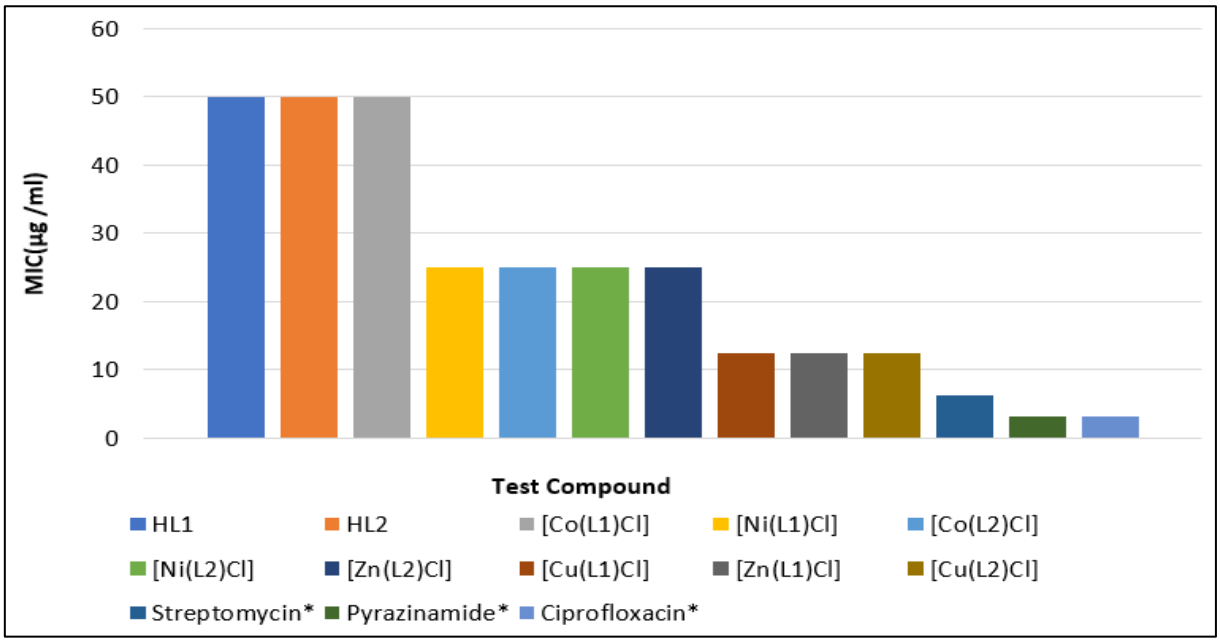

Fig 18 Structure of MIC (µg/ml) Values Test Compounds

V. CONCLUSION

The two unique Schiff bases and transition metal complexes were created. Several spectroscopic methods were used to assess these compounds. The Schiff base and ligand to metal ratio was 3:1 for the Co(III) complex and 2:1 for the Cu(II), Zn(II), and Ni(II) metal complexes, respectively, according to the physical and spectroscopic data. It has been speculated that cobalt complexes will exhibit octahedral geometry, nickel and copper complexes will have square planar geometry, and zinc complexes will have tetrahedral geometry. The biological activity investigations indicated that metallic compounds exhibited greater antitubercular and antimicrobial capabilities against M. tuberculosis, particularly against MBL and ESBL pathogenic bacteria, than corresponding parent ligands. Cobalt complex $[Co(L_1)Cl]$ and copper complex $[Cu(L_1)Cl]$. Whereas conventional copper complexes $[Cu(L_2)Cl]$ and $[Cu(L_1)Cl]$ and zinc complexes $[Zn(L_1)\ Cl]$ indicated strong anti-tubercular action, and compounds Ni(II) & Co(III) showed notable antibacterial activity. New lead compounds with more effective medicinal qualities may be synthesised as a result of this research, possibly contributing to the creation of metal-derived prescription drugs.

ACKNOWLEDGEMENT

The authors are highly grateful to our principal, Prof. C. K. Goutam, Agra College, Agra, DBRA, University, Agra, and Head Prof. Sanchita Singh, Dept. of Chemistry, for providing facilities in the Chemistry Laboratory and thankful to the Dept. of JNU Medical College, AMU, Aligarh; USIF, AMU, Aligarh for providing FTIR, EDX, UV-Vis, NMR, and research facilities. We would like to thank Beenesh Kumar Research scholar, and all the members of the research team, and we also want to express our gratitude to all of the anonymous reviewers for their insightful comments that permitted us to further refine the manuscript.

➢ *The Authorship Contribution Statement:*

Prof. Vipin Kumar Singh: Supervision, Investigation, Resources, writing review, and editing. Devendra Kumar Singh: Writing- original draft, Software execute, conceptualization, Result Analysis, Methodology. Bipin Bahadur Saxena: Software and Technical Lab Support

➢ *Inform Consent to Statements:*

All authors had been inform about this article or have agreed to read and publish this article.

➢ *Conflicts of Interest:*

No conflict of interest.

➢ *Ethics Declarations:*

Ethics approval and consent to participate

Not applicable.

REFERENCES

[1]. Patil, S.A.; Patil, R.; Patil, S.A. (2017) Recent Developments in Biological Activities of Indanones. Eur. J. Med. Chem. 138, 182–198. [Google Scholar] [CrossRef] [PubMed]

[2]. Turek, M.; Szczęsna, D.; Koprowski, M.; Bałczewski, P. (2017) Synthesis of 1-Indanones with a Broad Range of Biological Activity. Beilstein J. Org. Chem. 13, 451–494. [Google Scholar] [CrossRef] [PubMed]

[3]. Menezes, J.C.J.M.D.S. (2017) Arylidene Indanone Scaffold: Medicinal Chemistry and Structure–Activity Relationship View. RSC Adv. 7, 9357–9372.

[4]. Pluskota, R.; Koba, M.. (2018) Indandione and Its Derivatives—Chemical Compounds with High Biological Potential. Mini-Rev. Med. Chem. 18, 1321–1330. doi: 10.2174/1389557518666180330101809. [DOI] [PubMed] [Google Scholar]

ISSN No:-2456-2165 https://doi.org/10.38124/ijisrt/26jul1822

[5]. Z.H. Chohan and A. Rauf, (1992) Studies on biologically active complexes of cobalt(II) and nickel(II) with dithiooxamide-derived ligands. J. Inorg. Biochem., 46 (1), 41-48. https://doi.org/10.1016/0162-0134(92)80062-Z.

[6]. Z.A. Taha, A.K. Hijazi, W.M. Al Momani, (2020) Lanthanide complexes of the tridentate Schiff base ligand salicylaldehyde-2-picolinoylhydrazone: synthesis, characterization, photophysical properties, biological activities and catalytic oxidation of aniline, J. Mol. Struct. 1220. 128712, https://doi.org/10.1016/j.molstruc.2020.128712.

[7]. R. Malhotra, M. S. Malik, J. P. Singh, K. S. Dhindsa. (1992) Synthesis, characterization, and microbiocidal activity of α-methyl-(2-thiophenomethylene) aryloxyacetic acid hydrazides and their metal complexes. J. of Inor. Biochem. 45 (4), 269-275. https://doi.org/10.1016/0162-0134(92)84015-F.

[8]. Prem Ponka, Des Richardson, Erica Baker, Herbert M. Schulman, John T. Edward. (1988) Effect of pyridoxal isonicotinoyl hydrazone and other hydrazones on iron release from macrophages, reticulocytes and hepatocytes. Biochimica et Biophysica Acta (BBA) - General Subjects. 967 (1), 122-129. https://doi.org/10.1016/0304-4165(88)90197-3.

[9]. A.M. Ramadan. (1997) Structural and biological aspects of copper (II) complexes with 2-methyl-3-amino-(3 H)-quinazolin-4-one. Journal of Inorganic Biochemistry. 65 (3), 183-189. https://doi.org/10.1016/S0162-0134(96)00122-5.

[10]. Alessia Bacchi, Mauro Carcelli, Paolo Pelagatti, Corrado Pelizzi, Giancarlo Pelizzi, Franca Zani. (1999) Antimicrobial and mutagenic activity of some carbono- and thiocarbonohydrazone ligands and their copper(II), iron(II) and zinc(II) complexes. Journal of Inorganic Biochemistry. 75 (2), 123-133. https://doi.org/10.1016/S0162-0134(99)00045-8.

[11]. B. Bottari, R. Maccari, F. Monforte, R. Ottanà, E. Rotondo, M.G. Vigorita. (2000) Isoniazid-related copper(II) and nickel(II) complexes with antimycobacterial in vitro activity. Part 9. Bioorganic & Medicinal Chemistry Letters. 10 (7), 657-660. https://doi.org/10.1016/S0960-894X(00)00058-5.

[12]. B. Bottari, R. Maccari, F. Monforte, R. Ottanà, M.G. Vigorita, G. Bruno, F. Nicolò, A. Rotondo, E. Rotondo. (2001) Nickel(II) 2,6-diacetylpyridine bis(isonicotinoylhydrazonate) and bis(benzoylhydrazonate) complexes: structure and antimycobacterial evaluation. Part XI. Bioorganic & Medicinal Chemistry. 9 (8), 2203-2211. https://doi.org/10.1016/S0968-0896(01)00133-X.

[13]. A. Bagchi, P. Mukherjee, A. Raha, (2015) A review on transition metal complex-mordern weapon in medicine international journal of recent advances in pharmaceutical research a review on transition metal complex-mordern weapon in medicine, Bagchi Al Int. J. Recent Adv. Pharm. Res. 5 (3), 171–180.

[14]. M. Carcelli, P. Mazza, C. Pelizzi, F. Zani. (1995) Antimicrobial and genotoxic activity of 2,6-diacetylpyridine bis(acylhydrazones) and their complexes with some first transition series metal ions. X-ray crystal structure of a dinuclear copper(II) complex. Journal of Inorganic Biochemistry. 57 (1), 43-62. https://doi.org/10.1016/0162-0134(94)00004-T.

[15]. P. Mazza, F. Zani, M. Orcesi, C. Pelizzi, G. Pelizzi, G. Predieri. (1992) Synthesis, structure, antimicrobial, and genotoxic activities of organotin compounds with 2,6-diacetylpyridine nicotinoyl- and isonicotinoyl hydrazones. Journal of Inorganic Biochemistry. 48 (4), 251-270. https://doi.org/10.1016/0162-0134(92)84052-O.

[16]. S.K. Bharti, S.K. Singh. (2009) Metal based drugs: current use and future potential, Library (Lond). 1 (2), 39–51.

[17]. Du, H.; Williams, C.T.; Ebner, A.D.; Ritter, J.A. (2010) In situ FTIR spectroscopic analysis of carbonate transformations during adsorption and desorption of CO2 in K-promoted HTlc. Chem. Mater. 22, 3519–3526.

[18]. Heba Alshater, Ahlam I. Al-Sulami, Samar A. Aly, Ehab M. Abdalla ,Mohamed A. Sakr and Safaa S. Hassan. (2023) Antitumor and Antibacterial Activity of Ni(II), Cu(II), Ag(I), and Hg(II) Complexes with Ligand Derived from Thiosemicarbazones: Characterization and Theoretical Studies. Joun. Molecules . 28 (6), 2590. https://doi.org/10.3390/molecules28062590.

[19]. Albert A. (2012) Selective toxicity: the physico-chemical basis of therapy.7th edition. London: Springer Science & Business Media.

[20]. Efthimiadou EK, Sanakis Y, Katsaros N, Karaliota A, Psomas G. (2007) Transition metal complexes with the quinolone antibacterial agent pipemidic acid: synthesis, characterization and biological activity. Polyhedron. 26 (5): 1148-1158. https://doi.org/10.1016/j.poly.2006.10.017.

[21]. Bharti Sharma, Sudeep Shukla, Rohit Rattan, Musarrat Fatima, Mayurika Goel, Mamta Bhat, Shruti Dutta, Rakesh Kumar Ranjan, Mamta Sharma. (2022) Antimicrobial Agents Based on Metal Complexes: Present Situation and Future Prospects. Int. J. Biomater. 2022, 6819080. https://doi.10.1155/2022/6819080.

[22]. Kumar, B., Devi, J., Dubey, A. et al. (2023) Investigation of antituberculosis, antimicrobial, anti-inflammatory efficacies of newly synthesized transition metal(II) complexes of hydrazone ligands: structural elucidation and theoretical studies. Sci Rep 13, 15906. https://doi.org/10.1038/s41598-023-42180-4.

[23]. Chaudhary, R., Reddy, D., Sinha, A. and Kumar, A. (2024) Synthesis, characterization, antimicrobial and antitubercular evaluation of nickel (II) complexes of ON donor quinoline-hydrazide core. 78 (5), 1-10. https://doi.10.1007/s11696-024-03307-7.

[24]. Wildan Mubaraq, Indah Raya, Herlina Rasyid, Nunuk Hariani Soekamto, Hasnah Natsir, Djabal Nur Basir, Rizal Irfandi, Bulkis Musa1, Erna Mayasari,Wanda Wardyanti, Andi Adillah Nur Syafirah, Desy Kartina and Santi Santi. (2025) Exploration of Antituberculosis Potential of Ni(II) and Zn(II) Serine-

ISSN No:-2456-2165 https://doi.org/10.38124/ijisrt/26jul1822

Tyrosine Dithiocarbamate Complexes: Synthesis, Characterization, In Silico Profile, and In Vitro Evaluation. Trends in Sciences. 22(11), 10800. https://doi.org/10.48048/tis.2025.10800.

[25]. Kongot, M., Chaudhary, R., Reddy, D.S. et al. (2024) Synthesis, characterization, antimicrobial and antitubercular evaluation of nickel (II) complexes of ON donor quinoline-hydrazide core. Chem. Pap. 78, 3223–3232. https://doi.org/10.1007/s11696-024-03307-7.

[26]. Paison F, Su B, Pan D, Yan T and Wu J. (2020) The Study of Biological Activities of Various Mixed Ligand Complexes of Nickel(II). Austin Biochem. 5(1), 1025.

[27]. Priya P. Netalkar, Sandeep P. Netalkar & Vidyanand K. Revankar (2014) Nickel(II) complexes of thiosemicarbazones: synthesis, characterization, X-ray crystallographic studies and in vitro antitubercular and antimicrobial studies. Transition Metal Chemistry. 39, 519-526. https://doi.org/10.1007/s11243-014-9827-8.

[28]. Singh LR, Avula SR, Raj S, Srivastava A, Palnati GR, Tripathi CKM, Pasupuleti M, Sashidhara KV (2017) Coumarin–benzimidazole hybrids as a potent antimicrobial agent: synthesis and biological elevation. J Antibiot. https ://doi.org/10.1038/ja.2017.70.

[29]. WHO annual TB report (2025). http://apps.who.int/iris/bitst ream/10665 /25476 2/1/97892 90225 84-eng.pdf**.** Accessed 13 November 2025.

[30]. Patel RV, Patel PK, Kumari P, Rajani DP, Chikhalia KH (2012) Synthesis of benzimidazolyl-1,3,4-oxadiazol-2ylthio-N phenyl(benzothiazolyl) acetamides as antibacterial, antifungal and antituberculosis agents. Eur J Med Chem 53:41–51.

[31]. Bhalla AS, Goyal A, Guleria R, Gupta AK. (2015) Chest tuberculosis: radiological review and imaging recommendations. Indian J Radiol Imag. 25:21325. doi: 10.4103/0971-3026.161431

[32]. Natarajan A, Beena PM, Devnikar AV, Mali S. (2020) A systemic review on tuberculosis.Indian J Tuberc. 295–311. https://doi.10.1016/j.ijtb.2020.02.005.

[33]. Huang Y, Ai L, Wang X, Sun Z, Wang F. (2022) Review and updates on the diagnosis of tuberculosis. J Clin Med. 11:5826. https://doi.10.3390/jcm11195826.

[34]. Sharma SK, Mohan A, Kohli M. (2021) Extrapulmonary tuberculosis. Expert Rev Respir Med. 15:931–48. https://doi.10.1080/17476348.2021.1927718,

[35]. PaiM, BehrM, DowdyD, DhedaK, DivangahiM, BoehmeC, etal. (2016) Nature reviews disease primers. Tuberculosis. 2, 16076. https://doi.10.1038/nrdp.2016.76.

[36]. Cronan MR. (2022) In the thick of it: formation of the tuberculous granuloma and its effects on host and therapeutic responses. Front Immunol. 13:820134. https://doi.10.3389/fimmu.2022.820134.

[37]. Alsayed SS, Gunosewoyo H. (2023) Tuberculosis: pathogenesis, current treatment regimens and new drug targets. Int J Mol Sci. 24:5202. https://doi.10.3390/ijms24065202.

[38]. Qin Y, Chen Y, Chen J, Xu K, Xu F, Shi J. (2022) The relationship between previous pulmonary tuberculosis and risk of lung cancer in the future. Infect Agent Cancer.) 17, 20. https://doi.10.1186/s13027-022-00434-2.

[39]. HwangSY, KimJY, LeeHS, LeeS, KimD, KimS, etal. (2022) Pulmonary tuberculosis and risk of lung cancer: a systematic review and meta-analysis. J Clin Med. 11,765. https://doi.10.3390/jcm11030765.

[40]. Ho L-J, Yang H-Y, Chung C-H, Chang W-C, Yang S-S, Sun C-A, et al. (2021) Increased risk of secondary lung cancer in patients with tuberculosis: a nationwide, population based cohortstudy. PLoSONE.16:e0250531.https://doi.10.1371journal.pone.0250531.

[41]. TawfickMM, BadawyMSE, TalebMH, MenofyNGE.Tuberculosis diagnosis and detection of drug resistance: a comprehensive updated review. J Pure Appl Microbiol. (2023) 17:2849–66. https://doi.10.22207/JPAM.17.4.56.

[42]. MacGregor-Fairlie M, Wilkinson S, Besra GS, Goldberg Oppenheimer P. (2020) Tuberculosis diagnostics: overcomingancientchallenges withmodernsolutions.Emerg Top Life Sci. 4, 435–48. https://doi.10.1042/ETLS20200335.

[43]. WHO. Global Tuberculosis Report 2021, (2021). Available online at: https://www.who.int/publications/digital/global-tuberculosis-report-2021/tb-diagnosis treatment/treatment (Accessed March 11, 2025).

[44]. WHO.Global Tuberculosis Report 2023 (2023). Available online at: https://www. who.int/publications/i/item/9789240083851 [Accessed July 09, 2025].

[45]. Silva S, Arinaminpathy N, Atun R, Goosby E, Reid M. (2021) Economic impact of tuberculosis mortality in 120 countries and the cost of not achieving the sustainable development goals tuberculosis targets: a full-income analysis. Lancet Global Health. 9:e1372–e9. https://doi.10.1016/S2214-109X(21)00299-0.

[46]. Network GT, Casco N, Jorge AL, Palmero DJ, Alffenaar J-W, Fox GJ, et al. (2023) Long term outcomes of the global tuberculosis and COVID-19 co-infection cohort. Eur Respir J. 62:2300563. https://doi.10.1183/13993003.00563-2023.

[47]. García-García J-M, Blanc F-X, Buonsenso D, Centis R, Codecasa LR, D'Ambrosio L, et al. (2022) COVID-19 hampered diagnosis of TB infection in France, Italy, Spain and the United Kingdom. Arch Bronconeumol. 58, 783. https://doi.10.1016/j.arbres.2022.07.013.

[48]. Goletti D, Al-Abri S, Migliori GB, Arlehamn CL, Haldar P, Sundling C, et al. (2024) World tuberculosis day 2024 theme "Yes! We Can End Tb" can be made a reality through concerted global efforts that advance detection, diagnosis, and treatment of tuberculosis infection and disease. Int J Infect Dis. 141:106993. https://doi.10.1016/j.ijid.2024.106993.

[49]. Pandey J, Tiwari VK, Verma SS, Chaturvedi V, Bhatnagar S, Sinha S, Gaikwad AN, Tripathi RP (2009) Synthesis and antitubercular screening of

ISSN No:-2456-2165 https://doi.org/10.38124/ijisrt/26jul1822

imidazole derivatives. Eur J Med Chem 44:3350–3355.
[50]. B. Boehner, D. Dawes, W. Meyer, (1974) Synthesis and biological activity of new heterocyclic (thio) phosphates, Kem. Chem. J. 1 (9), 585–589.
[51]. R.P. Saini, V. Kumar, A.K. Gupta, G.K. Gupta, (2014) Synthesis, characterization, and antibacterial activity of a novel heterocyclic schiff's base and its metal complexes of first transition series, Med. Chem. Res. 23 (2), 690–698, https://doi.org/10.1007/s00044-013-0657-6.
[52]. V. Patel, P. Trivedi, H. Gohel, D. Khetani, (2014) Synthesis and characterization of schiff base of p - chloro aniline, their metal complexes and their evaluation for antibacterial activity, Int. J. Adv. Pharmacy, Biol. Chem. 3 (4), 999–1003.
[53]. HH, E. (2013) Synthesis, Characterization and antibacterial activity of macrocyclic schiff bases based on 1,3-docarbonyl phenyl dihydrazide, 1,4-docarbonyl phenyl dihydrazide, Org. Chem. Curr. Res. 2 (3), https://doi.org/10.4172/2161- 0401.1000122.
[54]. D.A. Xavier, N. Srividhya, (2014) Synthesis and study of schiff base ligands, IOSR J. Appl. Chem. 7 (11), 06–15, https://doi.org/10.9790/5736-071110615.
[55]. M. Zarei, A. Jarrahpour, (2011) Green and efficient synthesis of azo schiff bases, Iran. J. Sci. Technol. 35, 235–242.
[56]. Z. Yang, P. Sun, (2006) Compare of three ways of synthesis of simple schiff base, Molbank 2006 (6). https://doi.org/10.3390/M514.
[57]. A.S. El-tabl, M.M.A. Wahed, S.M. El-gamasy. (2016) Synthesis, structural characterization and study of some new antimicrobial action of metal complexes of (E) -N ', Yloxy), Acetohydrazonohydrazide Schiff Base 6 (June), 513–536.
[58]. L.A. Paquette. (1968) Principles of Modern Heterocyclic Chemistry, Benjamin.
[59]. M. Yoshizawa, T. Kusukawa, M. Kawano, T. Ohhara, I. Tanaka, K. Kurihara, N. Niimura, M. Fujita. (2005) Endohedral clusterization of ten water molecules into a "Molecular Ice" within the hydrophobic pocket of a self-assembled cage, J. Am. Chem. Soc. 127 (9), 2798–2799, https://doi.org/10.1021/ja043953w.
[60]. Lata S, Narasimhan B (2014) Biological activities of benzimidazole deriva tives in the new millennium. In: Narasimhan B (ed) 21st Century: the era of heterocyclic compounds in medicinal chemistry. Lambert Academic Publishing, Saarbrücken, pp 176–259
[61]. Yadav S, Narasimhan B, Lim SM, Ramasamy K, Vasudevan M, Shah SAA, Mathur A (2018) Synthesis and evaluation of antimicrobial, antitubercular and anticancer activities of benzimidazole derivatives. EJBAS 5:100–109.
[62]. Jones D H, Slack R, Squires S and Wooldridge K.R.H. (1965) Antiviral Chemotherapy. I. The Activity of Pyridine and Quinoline Derivatives against Neurovaccinia in Mice. J. Med. Chem. 8, 5, 676–680. https://doi.org/10.1021/jm00329a026.
[63]. Nazirkar, B., Mandewale, M. & Ramesh Yamgar, R. (2019) Synthesis, characterization and antibacterial activity of Cu (II) and Zn (II) complexes of 5-aminobenzofuran-2-carboxylate Schiff base ligands. Jour. of Taibah Uni. for Sci. 13 (1), 440-449. https;//doi.10.1080/1683655.2019.1592316.
[64]. Eliene Leandro de Araujo, Hellen Franciane Gonc, alves Barbosa, Edward Ralph Dockal, Eder Tadeu Gomes Cavalheiro. (2017) Synthesis, characterization and biological activity of Cu(II), Ni(II) and Zn(II) complexes of biopolymeric Schiff bases of salicylaldehydes and Chitosan. Int. Jour. of Biolog, Macromolec. 95, 168-176. http://dx.doi.org/10.1016/j.ijbiomac.2016.10.109.
[65]. Qiuyue, Zhang., Wenhua, Lin., Tian, Liu., Zhibin, Ye., Tongling, Liang and Wen-Hua Sun. (2021) Fluorinated Sterically Bulky Mononuclear and Binuclear 2-Iminopyridylnickel Halides for Ethylene Polymerization: Effects of Ligand Frameworks and Remote Substituents. ACS Omega. 6, 30157-30172. https://doi.org/10.1021/acsomega.1c05418.
[66]. Jha, P. K., Jha, I. K. and Mishra, P. M. (2005) Synthesis and characterization of some transition metal complexes with Schiff base. Asian Jour. of chem. 17 (4), 2239-2242.
[67]. Rao, C.N.R. and Venkataraghavan, R. (1962) The C = S stretching frequency and the "-N-C = S bands" in the infrared. Jour. of Spectrochimica Acta. 18(4), 541-547. https;//doi.org/10.1016/S0371-1951(62)80164-7.
[68]. Omyma A. M. Ali., Doaa, A. Nassar and Aml, A. A. Awad. (2021) Structural Characterization, thermal studies, fluorescence and optical properties of metal carbonyl derivatives of N_2O_2 Schiff Base**.** Jour. of Scientifi. Rese. in Sci. 38 (1), 164-186. https://doi.org/10.21608/JSRS.2021.210666.
[69]. Ramesh Yamgar, R., Mandewale, M. & Nazirkar, B. (2019) Synthesis, characterization and antibacterial activity of Cu (II) and Zn (II) complexes of 5-aminobenzofuran-2-carboxylate Schiff base ligands. Jour. of Taibah Uni. for Sci. 13 (1), 440-449. https;//doi.10.1080/1683655.2019.1592316.
[70]. Shelke, V.A., Jadhav, S.M., Patharkar, V.R., Shankarwar, S.G., Munde, A.S. and Chondhekar, T.K. (2012) Synthesis, spectroscopic characterization and thermal studies of some rare earth metal complexes of unsymmetrical tetradentate Schiff base ligand. Arabian Jour. of Chemi. 5, 501-507. https:// doi.10.106/j.arabjc.2010.09.018.
[71]. Eder Tadeu Gomes Cavalheiro. Eliene Leandro de Araujo, Hellen Franciane Gonc, alves Barbosa, Edward Ralph Dockal (2017) Synthesis, characterization and biological activity of Cu(II), Ni(II) and Zn(II) complexes of biopolymeric Schiff bases of salicylaldehydes and chitosan. Int. Jour. of Biolog. Macro. 95, 168-176. http://dx.doi.org/10.1016/j.ijbiomac.2016.10.109.
[72]. Aml, A. A. Awad., Doaa, A. Nassar and Omyma A. M. Ali. (2021) Structural Characterization, thermal studies, fluorescence and optical properties of metal carbonyl derivatives of N_2O_2 Schiff Base**.** Jour. of Scientifi. Rese. in Sci. 38 (1), 164-186. https://doi.org/10.21608/JSRS.2021.210666.

ISSN No:-2456-2165 https://doi.org/10.38124/ijisrt/26jul1822

[73]. Konstantionvi, S., Radovanovi, B., Caki, @Ivojin and Vesnavasi. (2003) Synthesis and characterization of Co(II), Ni(II), Cu(II) and Zn(II) complexes with 3-salicylidenehydrazono-2-indolinone. J. Serb. Chem.Soc. 68 (8–9), 641–647. UDC547.576+546.47+546.56+546.735.74+543.422.25:615.281. JSCS – 3072.

[74]. Achut, S. M., Amarnath, N. J., Sarika, M. J. and Trimbak, K. C. (2010) Synthesis, characterization and thermal study of some transition metal complexes of an asymmetrical tetradentate Schiff base ligand. Jour. Serb. Chem. Soc. 75 (3) 349–359. UDC 546.562'742'732'712'723'+542.913: JSCS-3967542.9+547.571+547.551:543.57.

[75]. Tunde, L., Yusuf, Segun D., Oladipo, Sizwe Zamisa, Hezekiel M. Kumalo, Isiaka A. Lawal, Monsurat M. Lawal, and Nonhlangabezo Mabuba. (2021) Design of New Schiff-Base Copper(II) Complexes: Synthesis, Crystal Structures, DFT Study, and Binding Potency toward Cytochrome P450 3A4. ACS Omega. 6, 13704−13718. https://doi.org/10.1021/acsomega.1c00906.

[76]. Cohen, A.B., (1975) The interaction of α-1-antitrypsin with chymotrypsin, trypsin and elastase, Biochimica et Biophysica Acta (BBA)-Enzymology, 391(1), 193-200.

[77]. Mishra, N., Poonia, K., Kumar, D. (2013) An overview of biological aspects of Schiff base metal complexes, Int. J. Adv. Res. Tech., 2(8), 52-66.

[78]. Brodowska, K., E. Łodyga-Chruścińska. (2014) Schiff bases-interesting range of applications in various fields of science, Chemik, 68.2, 129-134.

[79]. Ahlam, J., Abdul-Ghani and Khaleel, Asmaa M. N. (2009) Synthesis and Characterization of New Schiff Bases Derived fromN (1)-Substituted Isatin with Dithiooxamide and Their Co(II), Ni(II), Cu(II), Pd(II), and Pt(IV) Complexes. Bioinorganic Chemistry and Applications. 2009, Article ID 413175. https://doi.10.1155/2009/413175.

[80]. Laila, H., Abdel-Rahman, Maram, T., Basha, Badriah Saad Al-Farhan, Walaa Alharbi, Mohamed, R., Shehata, Noura O., Al Zamil and Doaa Abou El-ezz. (2023) Synthesis, Characterization, DFT Studies of Novel Cu(II), Zn(II), VO(II), Cr(III), and La(III) Chloro-Substituted Schiff Base Complexes: Aspects of Its Antimicrobial, Antioxidant, Anti-Inflammatory, and Photodegradation of Methylene Blue. *Molecules.***28,**4777. https://doi.org/10.3390/molecules28124777.

[81]. Aiyelabola, T.O. (2021) Syntheses, Characterization and Biological Activity of Novel Thiazoylazo Dye and Its Coordination Compounds. Adv. in Biolog. Chem. 11, 179-205. https://doi.org/10.4236/abc.2021.115013.

[82]. Cohen, A.B., (1975) The interaction of α-1-antitrypsin with chymotrypsin, trypsin and elastase, Biochimica et Biophysica Acta (BBA)-Enzymology, 391(1), 193-200.

[83]. Mishra, N., Poonia, K., Kumar, D. (2013) An overview of biological aspects of Schiff base metal complexes, Int. J. Adv. Res. Tech., 2(8), 52-66.

[84]. Brodowska, K., E. Łodyga-Chruścińska. (2014) Schiff bases-interesting range of applications in various fields of science, Chemik, 68.2, 129-134.

[85]. Singh, K., Thakur, R., Kumar, V. (2016) Co (II), Ni (II), Cu (II), and Zn (II) complexes derived from 4-[{3-(4-bromophenyl)-1-phenyl-1*H*-pyrazol-4-ylmethylene}-amino]-3-mercapto-6-methyl-5-oxo-1, 2, 4-triazine, Beni-Suef Univ. J. Basic Appl. Sci., 21-30.

[86]. World Health Organization, Global Tuberculosis Report, (2016). http://www.who.int/tb/publications/global_report/gtbr2016_executive_summary.pdf?ua=1

[87]. TB India, Revised National TB Control Programme Annual Status Report, (2016). http://tbcindia.nic.in/showfile.php?lid=3180.

[88]. Beyene, G., Tsegaye, W. (2011) Bacterial uropathogens in urinary tract infection and antibiotic susceptibility pattern in jimma university specialized hospital, southwest Ethiopia, Ethiop. J. Health Sci. 21(2), 141-146.

[89]. Haque, R., Akter, M.L., Salam, M.A. (2015) Prevalence and susceptibility of uropathogens: a recent report from a teaching hospital in Bangladesh, BMC research notes, 8(1), 416.

[90]. Oberoi, L., Singh, N., Sharma, P., Aggarwal, A., (2013) ESBL, MBL and Ampc β lactamases producing superbugs-Havoc in the intensive care units of Punjab India, J. Clin. Diagn. Res., 7(1), 70-3.

[91]. Deshmukh, D.G., Damle, A.S., Bajaj, J.K., Bhakre, J.B., Patwardhan, N.S. (2011) Metallo-β-lactamase-producing clinical isolates from patients of a tertiary care hospital, J. Lab. Physicians, 3(2), 93. CrossRef.

[92]. Haloi,P., Mandal,R.K., Barman, P. (2025) A new fluorinated Schiff base and its Cu(II), Co(II), and Zn(II) complexes: Spectral characterization, DNA binding, in-vitro biological assays and molecular docking study. Inorg. Chem. Commun. 182, Part 3, 115612. https://doi.org/10.1016/j.inoche.2025.115612.

[93]. Arya, V.P., Maurya, A.K., Modanawal, V.K., Siddharth Baranwal & Jaiswal, N. (2026) Synthesis, characterization, computational and biological investigation of Co(II), Ni(II) and Cu(II) complexes with 2-hydroxy-1-naphthaldehyde derived Schiff base ligand. Spring. Nat. Discov. Chem. 3, 223. https://doi.org/10.1007/s44371-026-00651-3.